International Journal of Applied Pharmaceutics

ISSN- 0975-7058 Vol 16, Special Issue 1, 2024

Original Article

PHARMACOINFORMATICS ANALYSIS OF MORUS MACROURA FOR DRUG DISCOVERY AND DEVELOPMENT

PURNAWAN PONTANA PUTRA[1*], AIYI ASNAWI[2], FARIZA HAMDAYUNI[3], ARFAN[4], LA ODE AMAN[5]

[1]Department of Pharmaceutical Chemistry, Faculty of Pharmacy, Universitas Andalas, Padang-25163, Indonesia. [2]Faculty of Pharmacy, Bhakti Kencana University, Bandung-40614, Indonesia. [3]Bachelor Program, Faculty of Pharmacy, Universitas Andalas, Padang-25163, Indonesia. [4]Department of Pharmaceutical Analysis and Medicinal Chemistry, Faculty of Pharmacy, Universitas Halu Oleo, Kendari-93132, Indonesia. [5]Department of Chemistry, Faculty of Sciences and Mathematics, Universitas Negeri Gorontalo, Gorontalo-96128, Indonesia

[*]Corresponding author: Purnawan Pontana Putra; [*]Email: purnawanpp@phar.unand.ac.id

Received: 10 Oct 2023, Revised and Accepted: 23 Nov 2023

ABSTRACT

Objective: Pharmacoinformatics is an innovative approach rapidly evolving in pharmaceutical research and drug development. This study focuses on analysing Morus macroura, a plant species with untapped pharmacological potential. This investigation aims to leverage pharmacoinformatics techniques to unveil the hidden potential of Morus macroura in drug discovery and development.

Methods: The study includes analyses of protein-protein interactions, deep learning docking, adsorption tests, distribution, metabolism, excretion, molecular dynamics simulations and free energy calculation using Molecular Mechanics Generalized Born Surface Area (MMGBSA).

Results: Nine active compounds were identified in Morus macroura, namely Andalasin A, Guangsangon K, Guangsangon L, Guangsangon M, Guangsangon N, Macrourone C, Mulberrofuran G, Mulberrofuran K, and Mulberroside C. These compounds exhibit protein-protein interaction activities against a cytochrome P450 monooxygenase that catalyses the conversion of C19 androgens. These plant compounds influence aromatase excess syndrome, deficiency, and ovarian dysgenesis. Regarding drug-likeness, Mulberroside C and Macrourone C demonstrated good absorption potential by adhering to Lipinski's rule of five. Deep learning docking simulations yielded affinity results of-9.62 kcal/mol for Guangsangon M,-10.44 kcal/mol for Macrourone C, and-10.99 kcal/mol for Guangsangon L. Subsequent molecular dynamics simulations indicated that Guangsangon L and Macrourone C remained stable during a 100 ns simulation.

Conclusion: Morus macroura interacts with important proteins, particularly CYP19A1, which might influence health conditions like aromatase excess syndrome and ovarian dysgenesis. These findings provide potential paths for addressing specific health issues and advancing drug development. Molecular dynamics simulations indicated that Guangsangon L and Macrourone C remained stable during simulation.

Keywords: Pharmacoinformatics, Morus macroura, Protein-protein interactions, Deep Learning docking, Molecular dynamics

DOI: https://dx.doi.org/10.22159/ijap.2024.v16s1.26 Journal homepage: https://innovareacademics.in/journals/index.php/ijap

INTRODUCTION

Drug discovery and development is a complex and time-consuming process that involves the identification of potential drug targets, the design and synthesis of drug candidates, and the evaluation of their efficacy and safety. In recent years, pharmacoinformatics has emerged as a powerful tool for drug discovery and development, enabling the rapid and efficient analysis of large amounts of data to identify potential drug candidates [1].

The significance of Morus macroura has grown due to its increased importance for its antioxidant and anti-inflammatory properties, as well as its high safety profile [2]. This plant is abundant in is prenylated flavonoids and Diels–Alder type adducts with both structural and biological significance [3]. Researchers have explored both the fruits and leaves of Morus macroura Miq. as a potential source of bioactive compounds for addressing Alzheimer's disease (AD). Chemical profiling of their extracts has revealed a rich variety of phytochemicals [4]. The comprehensive spectrum of Morus macroura's activities demands deeper analysis

Notably, Morus Macroura contains key active compounds, andalasin A and mulberroside C, which have been extracted from its wood and exhibit weak antinematodal and moderate antifungal properties [5]. However, the diverse activities of Morus macroura need to be analyzed using pharmacoinformatics to understand the extent of Protein-Protein Interaction (PPI) influence on its usage. These PPIs could potentially serve as drug targets. Pharmacoinformatics can be employed to analyze these PPIs and identify the most promising drug targets. It is also essential to assess the drug-likeness of active compounds in Morus macroura to predict their absorption, distribution, metabolism, and excretion properties. This research aims to emphasize the need for a more profound exploration of Morus macroura's activities and how leveraging pharmacoinformatics, particularly in understanding PPIs, can uncover potential drug targets and assess the suitability of active compounds for further drug development.

Two commonly used databases for pharmacoinformatics research are the Kyoto Encyclopedia of Genes and Genomes (KEGG) and Online Mendelian Inheritance in Man (OMIM). KEGG disease pathways can help identify molecular pathways associated with specific diseases [6]. These pathways may offer potential drug targets. OMIM is a database that contains information about human genes and genetic diseases, aiding in the identification, design, and testing of drug targets [7]. Molecular docking simulations with deep learning can be utilized to investigate interactions between active compounds and proteins, while molecular dynamics simulations are necessary to assess the stability of the binding between active compounds and proteins. This study aims to provide a holistic understanding of the pharmacological effects of Morus macroura on proteins and genes for future drug development.

MATERIALS AND METHODS

Potential target analysis

In the pursuit of target prediction, the PhytoChemical Interactions DB (PCIDB), which can be accessed at https://www.genome.jp/db/pcidb/kna_species/6819. Concurrently, gene annotations relevant to human diseases were obtained from the National Center for Biotechnology Information (NCBI), accessible through this link: https://www.ncbi.nlm.nih.gov/gene/. To delineate potential Morus macroura targets associated with diseases, we considered overlapping targets. To identify significant disease-related target groups, we relied on protein-protein interaction (PPI) data

sourced from STRING, accessible at https://string-db.org/. Our focus organism was "Homo sapiens," and a stringent threshold of a score greater than 0.900 with a size cutoff exceeding 10 was applied [8].

ADMET analysis

We assessed the ADME (Absorption, Distribution, Metabolism, and Excretion) analysis of the compounds derived from Morus macroura, with potential application as pharmaceuticals. Our study involved utilizing the SWISS-ADME web server for predicting the ADME profile, accessible at http://www.swissadme.ch/. This server provides essential parameters encompassing lipophilicity, aqueous solubility, pharmacokinetic properties, and drug-likeness criteria [9].

Deep learning docking

Proteins and ligands were separated using Discovery Studio 2020 software, available at https://discover.3ds.com/. Geometric optimization was carried out using Avogadro software, with the Merck Molecular Force Field (MMFF94) serving as the force field. The receptor utilized in these simulations was the structure of human placental aromatase cytochrome P450 in complex with androstenedione, identified by its PDB ID: 3EQM [10]. Molecular docking simulations were performed using Python-based cloud computing on Google Colab [11]. For molecular docking simulations, the Deep Learning algorithm (Convolutional Neural Network) was implemented using Gnina software, version 1.0.3 [12, 13]. The grid box was established using the autobox ligand file to determine the binding site, which involved creating a prism around the ligand, with additional spacing in each dimension.

Molecular dynamics and free energy calculation

The protein employed was the structure of human placental aromatase cytochrome P450 in a complex with androstenedione, identified by its PDB ID: 3EQM [10]. Input file preparation and homology modeling were conducted using CHARMM-GUI [14]. Ionization was achieved using NaCl at a concentration of 0.15 M. The system employed Periodic Boundary Conditions with Particle-Mesh Ewald (PME) and Fast Fourier Transform (FFT). The CHARMM36M force field was applied to both the protein and ligand [15] and the TIP3P water model was used [16]. Hydrogen mass repartitioning was performed [16]. The equilibration process involved the NVT ensemble, followed by production simulations with the NPT ensemble at a temperature of 310 K. All simulations were executed using Gromacs 2023.1 software, with a total simulation time of 100 ns [17, 18]. Free energy calculations were carried out using gmx_MMPBSA [19].

RESULTS

The PPI networks to identify significant disease-related target groups for Homo sapiens organism (Fig. 1).

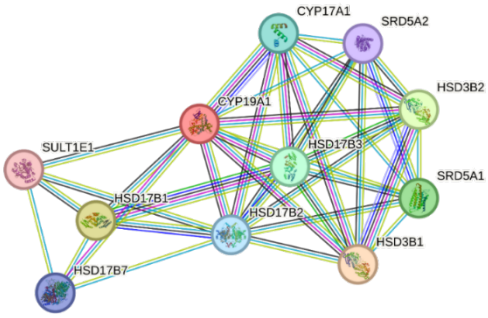

Fig. 1: Protein-protein interaction network derived from morus macroura

The study of ADME (Absorption, Distribution, Metabolism, and Excretion) properties of bioactive compounds is critical in drug development and understanding the pharmacokinetics of natural products. Morus macroura, a plant known for its medicinal properties, contained several compounds with diverse ADME characteristics. The study investigated the ADME properties of eight Morus macroura compounds, focusing on their lipophilicity, gastrointestinal absorption, and interactions with key CYP enzymes (table 1). The Log S values indicated the lipophilicity of the compounds. Compounds such as Andalasin A, Guangsangon K, and Mulberrofuran K had very low Log S values, indicating poor solubility. On the other hand, Mulberroside C had a higher Log S value, indicating better solubility. All compounds exhibited low GI absorption, which suggested that these compounds faced challenges in crossing the intestinal barrier and getting into the bloodstream, impacting their bioavailability. The interactions with CYP enzymes were crucial for understanding the potential for drug-drug interactions. Among the compounds, Guangsangon L and Macrourone C interacted with CYP2C9 and CYP3A4, indicating a potential for metabolism interactions. It's noteworthy that most of the compounds did not interact with several CYP enzymes, suggesting a reduced likelihood of interactions with drugs metabolized by these enzymes.

Table 1: The ADME properties of the morus macroura compounds

Compounds	Log S (ESOL)	GI Absorption	CYP1A2	CYP2C19	CYP2C9	CYP2D6	CYP3A4
Andalasin A	-6.13; Poorly soluble	Low	No	No	Yes	No	No
Guangsangon K	-6.52; Poorly Soluble	Low	No	No	No	No	No
Guangsangon L	-5.54; Moderately Soluble	Low	No	No	Yes	No	Yes
Guangsangon M	-6.77; Poorly Soluble	Low	No	No	No	No	No
Guangsangon N	-6.77; Poorly Soluble	Low	No	No	No	No	No
Macrourone C	-7.50; Poorly Soluble	Low	No	No	No	No	Yes
Mulberrofuran G	-7.44; Poorly Soluble	Low	No	No	No	No	No
Mulberrofuran K	-8.60; Poorly Soluble	Low	No	No	No	No	No
Mulberroside C	-3.79; Soluble	Low	No	No	No	No	No

Table 2: Lipinski's rule estimation of the morus macroura compounds

Compounds	Molecular weight (≤ 500) (g/mol)	MLOGP (≤ 4.15) (log $P_{o/w}$)	Num. H-bond acceptors (≤ 10)	Num. H-bond donors (≤ 5)	Lipinski rule
Andalasin A	488.49	2.20	8	8	Yes; 1 violation: NhorOH>5
Guangsangon K	626.61	0.68	11	8	No: 3 violation: MW>500, NorO>10, NHorOH>5
Guangsangon L	476.47	1.14	8	6	Yes: 1 violation: NhorOH>5
Guangsangon M	610.61	1.44	10	7	No: 2 violation: MW>500, NHorOH>5
Guangsangon N	610.61	1.44	10	7	No: 2 violation: MW>500, NhorOH>5
Macrourone C	492.60	3.19	6	4	Yes; 0 violation
Mulberrofuran G	562.57	3.21	8	5	Yes: 1 violation: MW>500
Mulberrofuran K	628.67	4.03	8	4	Yes: 1 violation: MW>500
Mulberroside C	458.46	-0.08	9	5	Yes; 0 violation

Lipinski's Rule of Five, developed by Christopher Lipinski, was a widely used guideline in drug discovery to assess the drug-likeness and pharmacokinetic properties of small molecules. It stated that for a compound to have good oral bioavailability, it should meet specific criteria related to molecular weight, lipophilicity (log P), the number of hydrogen bond acceptors, and the number of hydrogen bond donors (table 2). The study evaluated the suitability of eight Morus macroura compounds using Lipinski's Rule of Five, aiding in the prediction of their potential as potential drug candidates. Out of the eight compounds from Morus macroura, only Macrourone C and Mulberroside C fully complied with Lipinski's Rule of Five, with no violations. Andalasin A, Guangsangon L, Mulberrofuran G, and Mulberrofuran K met most of the criteria but had one violation each. Guangsangon K, Guangsangon M, and Guangsangon N each had multiple violations, making them less likely to be considered good drug candidates according to Lipinski's Rule.

Administration, distribution, metabolism, and elimination (ADME) radar parameters of Morus macroura compounds with provides essential parameters encompassing lipophilicity, aqueous solubility, pharmacokinetic properties, and drug-likeness criteria (fig. 2).

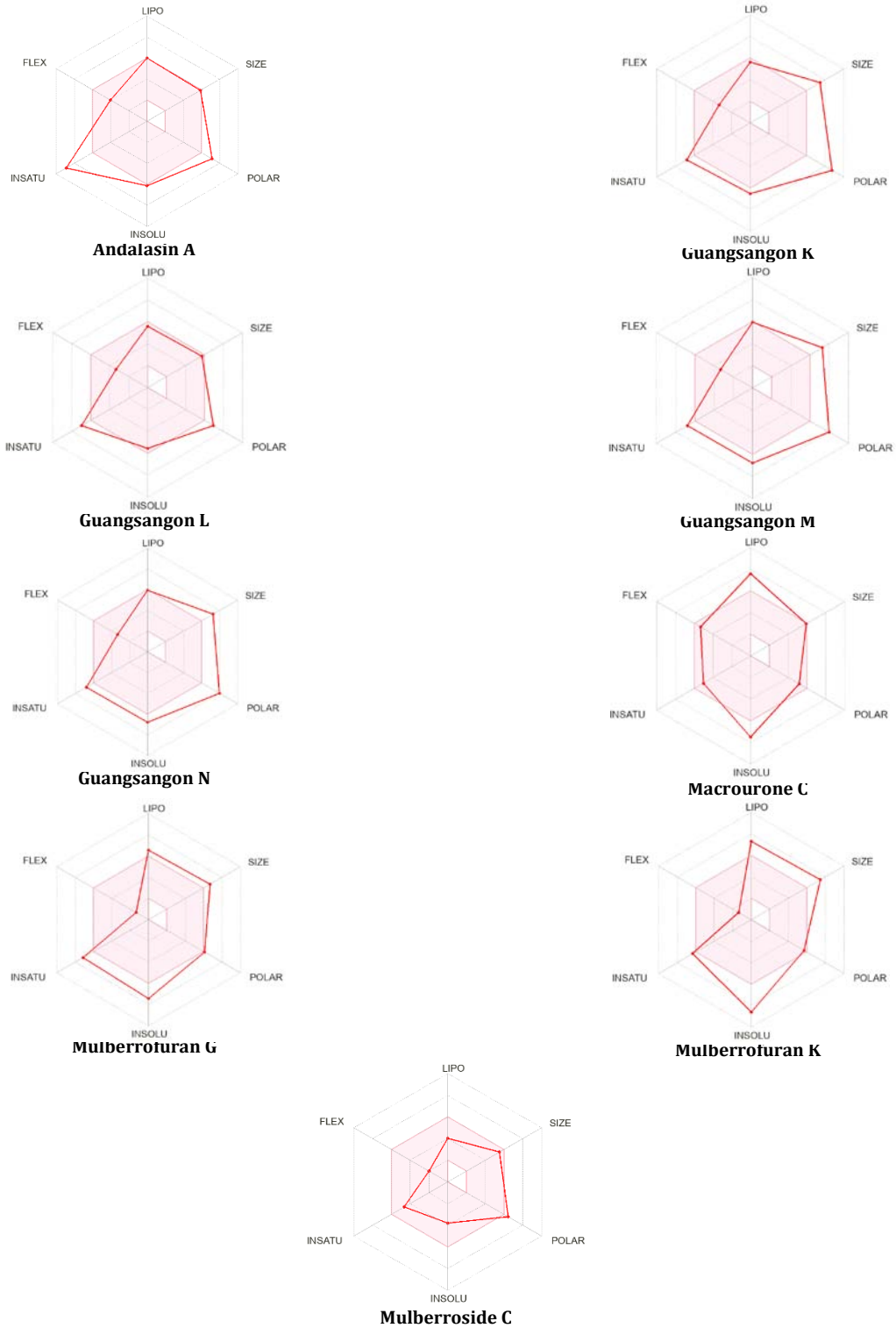

Fig. 2: Administration, distribution, metabolism, and elimination (ADME) radar parameters of Morus macroura compounds

In deep learning docking, the affinity and CNN Pose Score are crucial parameters for assessing the interactions between compounds and their target proteins. These metrics help in understanding the binding strength and pose accuracy of the ligands (table 3). We analyze the affinity and CNN Pose Scores of various compounds, including Andalasin A, Guangsangon K, Guangsangon L, Guangsangon M, Guangsangon N, Macrourone C, Mulberrofuran G, Mulberrofuran K, Mulberroside C, and the native ligand. Andalasin A exhibited an affinity of -5.32 kcal/mol, indicating a moderately strong binding to its target protein. Guangsangon K showed a slightly stronger binding affinity with a score of -6.26 kcal/mol compared to Andalasin A. Guangsangon L displayed the highest affinity among the listed compounds with a score of-10.99 kcal/mol, suggesting a strong and favorable binding interaction. Guangsangon M and Guangsangon N had affinity scores of -9.62 and -8.39 kcal/mol, respectively, indicating relatively strong binding interactions. Macrourone C also showed a high affinity score of -10.44 kcal/mol, similar to Guangsangon L. In contrast, Mulberrofuran G and Mulberrofuran K exhibited positive values of 5.88 and 0.38 kcal/mol, respectively. These positive values suggest repulsive interactions or poor binding affinity. Mulberroside C displayed an affinity of -8.93 kcal/mol, indicating a strong binding affinity similar to several other compounds on the list. The native ligand had an affinity of -10.68 kcal/mol, indicating a strong and favorable binding interaction, similar to Guangsangon L and Macrourone C.

The CNN Pose Score is a measure of how accurately the ligand has docked in the binding site of the target protein. A score closer to 1.0 suggests a more accurate pose. Andalasin A had a CNN Pose Score of 0.5631, indicating a reasonably accurate pose prediction. Guangsangon K exhibited a score of 0.4346, which suggests a less accurate binding pose prediction. Guangsangon L displayed a CNN Pose Score of 0.7654, indicating a relatively accurate binding pose prediction. Guangsangon M and Guangsangon N had scores of 0.5154 and 0.6154, respectively, suggesting moderately accurate pose predictions. Macrourone C had a CNN Pose Score of 0.6008, indicating a moderately accurate binding pose. Mulberrofuran G and Mulberrofuran K had scores of 0.4531 and 0.4086, respectively, suggesting less accurate pose predictions. Mulberroside C exhibited a CNN Pose Score of 0.6117, indicating a moderately accurate binding pose prediction. The native ligand had the highest CNN Pose Score on the list, with a score of 0.9104, indicating a highly accurate binding pose prediction.

In summary, the affinity values reveal the strength of binding interactions, with Guangsangon L, Macrourone C, Guangsangon L and the native ligand showing strong affinities. The CNN Pose Scores provide insights into the accuracy of ligand binding poses, where the native ligand, Guangsangon L, and Macrourone C demonstrated relatively accurate binding predictions. These results are essential for understanding the potential of these compounds as drug candidates or for further optimization in drug discovery processes.

Table 3: Molecular docking simulation results

Compounds	Affinity (kcal/mol)	CNN pose score	Hydrogen interaction	Hydrophobic interaction
Andalasin A	-5.32	0.5631	Ser478, Met374, Leu372. Arg115	Ile133, Ala438, Ala306, Val370, Thr310, Leu477
Guangsangon K	-6.26	0.4346	Cys437, Ser478	Val373, Val370, Phe134, Ile133, Ala306, Val313
Guangsangon L	-10.99	0.7654	Leu477, Arg115, Met374, Pro429, Ala438	Trp224, Ala438, Ile133
Guangsangon M	-9.62	0.5154	Ile132, Trp141, Arg435, Gly436	Ala306, Ile133, Phe430, Val370, Val373
Guangsangon N	-8.39	0.6154	Cys 437, Leu477, Asp309	Phe430, Val370, Thr310, Ile133
Macrourone C	-10.44	0.6008	Arg115, Ala438	Val370, Trp224, Ile133, Ala306, Leu152, Cys437, Ala443
Mulberrofuran G	5.88	0.4531	Arg115, Arg145	Ile70, Ile133, Ile132, Ala438, Cys437, Val373, Phe430, Val370, Ala306
Mulberrofuran K	0.38	0.4086	Ser478, Cys437	Val370, Val373, Phe134, Ile133, Cys437, Ala306, Val313
Mulberroside C	-8.93	0.6117	Leu477, Met374, Gly431	Val370, Phe430, Cys437, Val373
Native ligand	-10.68	0.9104	Arg115, Met374, Ala306	Trp224

Information

CNN: Conventional Neural Networks

The binding mode of Guangsangon L, Guansangon M, Macrourone C, and Native Ligand show a similar pattern trend in molecular docking simulation (fig. 3).

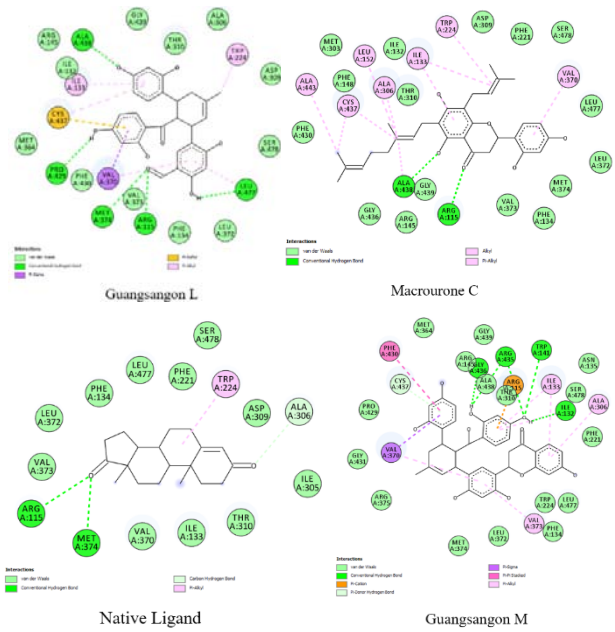

Fig. 3: The interactions that occur between Guangsangon L, Guangsangon M, and Macrourone C. These 3 compounds have the minimum affinity

Table 4: Free energy calculation results using the generalized born and surface area solvation (MMGBSA) approach

Compounds	ΔG (kcal/mol)
Guangsangon L	-31.47±2.51
Guangsangon M	-47.20±2.69
Macrourone C	-40.44±1.60
Native Ligand	-24.00±1.56

The RMSD values of Guangsangon L, Guansangon M, Macrourone C, and Native Ligand illustrated the bond stability for 100 ns simulation (fig. 4).

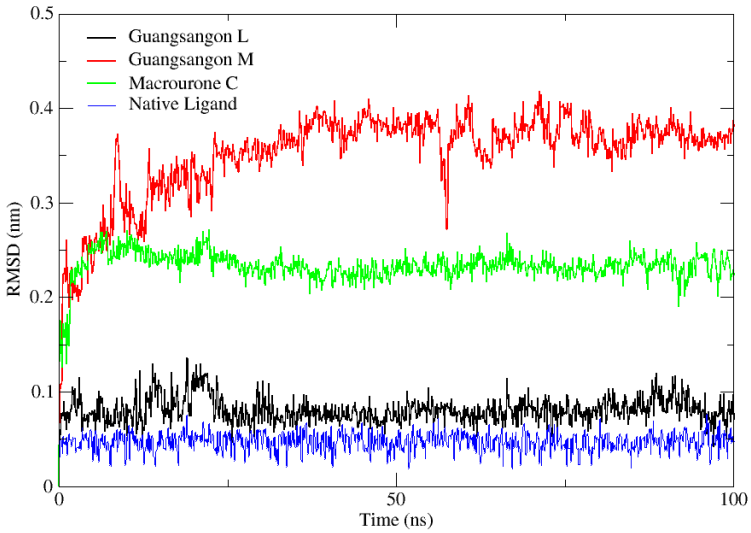

Fig. 4: RMSD values for 100 ns Guangsangon L (Black), Guansangon M (Red), Macrourone C (Green) and Native Ligand (Blue), illustrate the bond stability during the simulation, The RMSD values of Guangsangon L, Macrourone C, and Native Ligand show a similar pattern trend for 100 ns simulation (fig. 4)

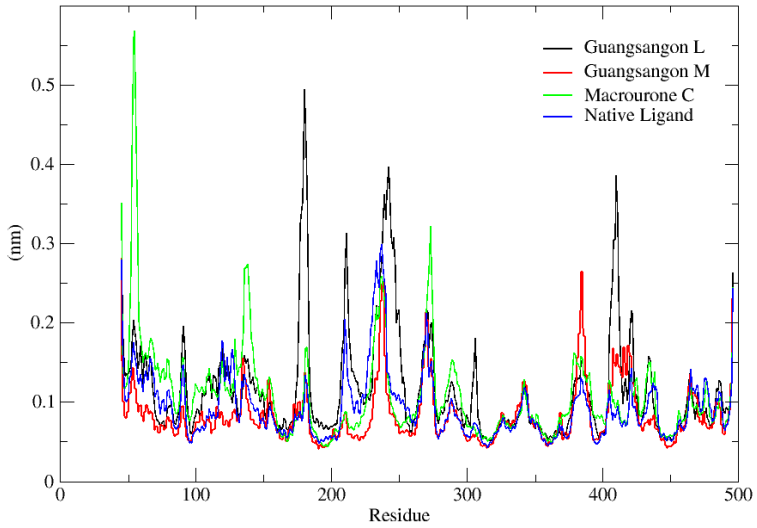

Fig. 5: RMSF values for 100 ns Guangsangon L (Black), Guansangon M (Red), Macrourone C (Green) and Native Ligand (Blue), depict the amino acids that experienced fluctuations in the simulation.

DISCUSSION

Morus macroura exhibits protein-protein interactions with A cytochrome P450 monooxygenase, namely CYP19A1, which catalyzes the conversion of C19 androgens. CYP19A1 is linked to other proteins or genes, with green lines denoting gene neighborhood interactions, red signifying gene fusions, blue indicating gene co-occurrence, black lines representing co-expression connections, and purple indicating homologous associations. The predicted functional partners interconnected in this network include 3 beta-hydroxysteroid dehydrogenase (HSD3B1), Estradiol 17-beta-dehydrogenase 1 (HSD17B1), 3 beta-hydroxysteroid dehydrogenase (HSD3B2), 3-oxo-5-alpha-steroid 4-dehydrogenase 1 (SRD5A1), Testosterone 17-beta-dehydrogenase 3 (HSD17B3), Steroid 17-alpha-hydroxylase (CYP17A1), Estradiol 17-beta-dehydrogenase 2 (HSD17B2), 3-keto-steroid reductase (HSD17B7), 3-oxo-5-alpha-steroid 4-dehydrogenase 2 (SRD5A2), and Sulfotransferase 1E1 (SULT1E1) (fig. 1). These functional partners encompass not only physically linked proteins within a protein complex or involved in temporary interactions but also those with more indirect associations [20]. Furthermore, data from KEGG Disease and OMIM indicate that this plant affects aromatase excess syndrome, deficiency, and ovarian dysgenesis.

We delved into the ADME (Absorption, Distribution, Metabolism, and Excretion) prediction results concerning the compounds from Morus macroura (table 1). Interestingly, Mulberroside C displayed notably good solubility within a range of values from-3.05 to-3.92. Solubility is a pivotal factor in drug development, dictating how effectively a compound can dissolve in bodily fluids and subsequently be absorbed by the body. This attribute bodes well for the compound's potential in the drug development process, as it can enhance its effectiveness and ability to traverse various stages, from formulation to successful absorption within the body [21, 22]. Furthermore, our analysis also spotlighted Guangsangon L, another compound from Morus macroura, which demonstrated moderate solubility, registering a value of-5.54. Although not as high as the solubility exhibited by Mulberroside C, moderate solubility remains favorable for drug development, suggesting that the compound can still perform effectively in its intended role.

Unfortunately, all identified compounds in Morus macroura exhibited low GI (Gastrointestinal) absorption, implying that these compounds might not be readily absorbed through the gastrointestinal tract, which could have implications for their bioavailability and distribution in the body [23]. These findings shed valuable light on the potential of these compounds for drug development and their impact on therapeutic effectiveness.

The compounds Andalasin A, Guangsangon L, and Macrourone C have distinctive interactions with the enzymes CYP2C9 and CYP3A4, which belong to the critical cytochrome P450 (CYP) family. These enzymes hold paramount importance in drug metabolism and elimination from the body. While Andalasin A and Guangsangon L are believed not to hinder CYP2C9's functionality, their presence doesn't significantly interfere with the drug pathways managed by this enzyme. Conversely, Macrourone C might inhibit the CYP3A4 enzyme, a key player in metabolizing many drugs. Such inhibition can lead to pronounced alterations in drug metabolism, potentially elevating drug concentrations within the body [24, 25].

Specifically, the compounds only Macrourone C and Mulberroside C fully complied with Lipinski's Rule of Five adhere to Lipinski's rules, as indicated in table 2. Lipinski's criteria serve as a foundational framework for assessing the potential of molecules to be orally active drugs, particularly concerning solubility and absorption [26]. Conversely, another molecule of interest, Mulberroside C, stands out for its conformity with Lipinski's criteria, positioning it as a favorable candidate in oral drug development. It's pivotal to report that compounds adhering to these criteria typically exhibit enhanced bioavailability, thereby increasing their potential efficacy and safety when administered orally.

The ADME (Absorption, Distribution, Metabolism, and Excretion) profile of compounds derived from Morus macroura is augmented with a radar chart, meticulously delineating six pivotal ADME parameters with a compound's potential for oral bioavailability. These parameters include LIPO (lipophilicity), SIZE (size), POLAR (polarity), INSOLU (insolubility), INSATU (instauration), and FLEX (flexibility), as elegantly illustrated in fig. 2. The colored sectors within the chart specify the domains of chemical features served for facilitating oral bioavailability. In a profound explanation gleaned from the ADME profile analysis, the compounds Mulberroside C and Guangsangon L emerge as exemplars of congruence across all parameters, encompassing the realms of lipophilicity, size, polarity, insolubility, saturation, and flexibility.

Molecular docking simulations, among these compounds, Guangsangon L exhibited the highest affinity with a score of-10.99 kcal/mol and displayed a strong interaction involving several amino acids, including Leu477, Arg115, Met374, Pro429, and Ala438 (fig. 3) and conventional Neural Networks (CNN) Pose Score of 0.7654. The closer this value approaches 1, the more closely it resembles the binding shape of the native ligand (table 3). Additionally, two compounds displayed positive affinities, indicating that the reactions wouldn't occur spontaneously, as observed in Mulberrofuran G and Mulberrofuran K. Positive affinity values also suggest unstable bonding. Three compounds, Guangsangon M, Macrourone C, and Guangsangon L, were predicted to have strong affinities for Aromatase cytochrome P450, and further molecular dynamics simulations were conducted (fig. 4 and 5). These simulations are crucial for understanding the stability of interactions between the ligand and receptor.

Molecular docking can provide a static representation of the ligand-receptor interactions, while molecular dynamics offers insight into dynamic interactions. Both molecular docking and molecular dynamics simulations employed data from the native ligand (4-Androstene-3-17-Dione) for validation and evaluation purposes. The simulations with the native ligand provided information about ligand potential, interaction identification, and mechanistic insights.

The results of the molecular dynamics simulations indicated that Guangsangon L and Macrourone C remained stable during a 100 ns simulation, as evidenced by Root Mean Square Deviation (RMSD) data (fig. 4). Root-Mean-Square Fluctuation (RMSF) data were used to assess protein flexibility and identify crucial residues for protein function (fig. 5).

Finally, binding stability analysis was performed using the Generalized Born and Surface Area Solvation (MMGBSA) method. Guangsangon M and Macrourone C exhibited the lowest ΔG energies (table 4). A lower ΔG value in free energy calculations signifies a higher affinity of the ligand for the drug target. Affinity measures the strength of the interaction between the ligand and the drug target, and a lower ΔG value indicates a stronger interaction. MMGBSA combines molecular mechanics (MM) with the Generalized Born Surface Area (GBSA) model to predict ligand affinity for the drug [27].

CONCLUSION

Morus macroura exhibits complex protein-protein interactions, particularly with CYP19A1, and has potential implications for diseases such as aromatase excess syndrome and ovarian dysgenesis. All compounds displayed low GI absorption, which may affect their bioavailability. Some compounds that meet the standards for making drugs that can be taken by mouth, such as Mulberroside C and Macrourone C. Deep learning docking simulations yielded affinity results of-9.62 kcal/mol for Guangsangon M,-10.44 kcal/mol for Macrourone C, and-10.99 kcal/mol for Guangsangon L. Following the molecular dynamics simulation, it was observed that Guangsangon L and Macrourone C maintained stability throughout a 100 ns simulation.

ACKNOWLEDGMENT

We sincerely appreciate the support, guidance, and financial assistance the Faculty of Pharmacy Universitas Andalas.

FUNDING

Faculty of Pharmacy Universitas Andalas

AUTHORS CONTRIBUTIONS

Purnawan Pontana Putra was responsible for conceptualization, data curation, investigation, methodology, visualization, and the creation of the initial written draft, as well as reviewing and editing. Aiyi Asnawi contributed to the methodology, investigation of Molecular Dynamics, and software-related tasks. Fariza Hamdayuni was involved in the methodology. Arfan handled the analysis of absorption, distribution, metabolism, and excretion, along with visualization. La Ode Aman took charge of interpreting the molecular dynamics.

CONFLICT OF INTERESTS

The authors have no known competing interests that could call into question the objectivity of this research.

REFERENCES

1. Nyola N, Jeyablan G, Kumawat M, Sharma R, Singh G, Kalra N. Pharmacoinformatics: a tool for drug discovery. Am J PharmTech Res. 2012;2(23).
2. Salama RM, Darwish SF, El Shaffei I, Elmongy NF, Fahmy NM, Afifi MS. Morus macroura Miq. Fruit extract protects against acetic acid-induced ulcerative colitis in rats: novel mechanistic insights on its impact on miRNA-223 and on the

TNFα/NFκB/NLRP3 inflammatory axis. Food Chem Toxicol. 2022;165. doi: 10.1016/j.fct.2022.113146.

3. Dai SJ, Mi ZM, Ma ZB, Li S, Chen RY, Yu DQ. Bioactive diels-alder type adducts from the stem bark of morus macroura. Planta Med. 2004;70(8):758-63. doi: 10.1055/s-2004-827208, PMID 15368673.
4. El-Hawary SS, Sayed AM, Issa MY, Ebrahim HS, Alaaeldin R, Elrehany MA. Anti-Alzheimer chemical constituents of morus macroura Miq: chemical profiling, in silico and *in vitro* investigations. Food Funct. 2021;12(17):8078-89. doi: 10.1039/D1FO01177D.
5. Syah YM, Achmad SA, Ghisalberti EL, Hakim EH, Iman MZN, Makmur L. Andalasin A, a new stilbene dimer from Morus macroura. Fitoterapia. 2000;71(6):630-5. doi: 10.1016/s0367-326x(00)00221-5, PMID 11077168.
6. Kanehisa M, Sato Y, Furumichi M, Morishima K, Tanabe M. New approach for understanding genome variations in KEGG. Nucleic Acids Res. 2019;47(D1):D590-5. doi: 10.1093/nar/gky962, PMID 30321428.
7. Amberger JS, Bocchini CA, Schiettecatte F, Scott AF, Hamosh A. OMIM.org: online mendelian inheritance in man (OMIM®), an online catalog of human genes and genetic disorders. Nucleic Acids Res. 2015;43:D789-98. doi: 10.1093/nar/gku1205, PMID 25428349.
8. Patel DA, Patel AC, Nolan WC, Huang G, Romero AG, Charlton N. High-throughput screening normalized to biological response: application to antiviral drug discovery. J Biomol Screen. 2014;19(1):119-30. doi: 10.1177/1087057113496848, PMID 23860224.
9. Daina A, Michielin O, Zoete V. Swiss ADME: a free web tool to evaluate pharmacokinetics, drug-likeness and medicinal chemistry friendliness of small molecules. Sci Rep. 2017;7:42717. doi: 10.1038/srep42717, PMID 28256516.
10. Ghosh D, Griswold J, Erman M, Pangborn W. Structural basis for androgen specificity and oestrogen synthesis in human aromatase. Nature. 2009;457(7226):219-23. doi: 10.1038/nature07614.
11. Bisong E. Google colaboratory. Build Mach Learn Deep Learn Model Google Cloud Platf; 2019. p. 59-64.
12. McNutt AT, Francoeur P, Aggarwal R, Masuda T, Meli R, Ragoza M. GNINA 1.0: molecular docking with deep learning. J Cheminform. 2021;13(1):43. doi: 10.1186/s13321-021-00522-2, PMID 34108002.
13. Rahim F, Putra PP, Ismed F, Putra AE, Lucida H, Molecular Dynamics. Docking and prediction of absorption, distribution, metabolism and excretion of lycopene as protein inhibitor of Bcl2 and DNMT1. Trop J Nat Prod Res. 2023;7:3439-44.
14. Lee J, Hitzenberger M, Rieger M, Kern NR, Zacharias M, Im W. Charmm-gui supports the amber force fields. J Chem Phys. 2020;153(3):035103. doi: 10.1063/5.0012280, PMID 32716185.
15. Huang J, Rauscher S, Nawrocki G, Ran T, Feig M, De Groot BL. Charmm36m: an improved force field for folded and intrinsically disordered proteins. Nat Methods. 2017;14(1):71-3. doi: 10.1038/nmeth.4067, PMID 27819658.
16. Mark P, Nilsson L. Structure and dynamics of the TIP3P, SPC, and SPC/E water models at 298 K. J Phys Chem A. 2001;105(43):9954-60. doi: 10.1021/jp003020w.
17. Handayani D, Aminah I, Pontana Putra P, Eka Putra A, Arbain D, Satriawan H. The depsidones from marine sponge-derived fungus aspergillus unguis IB151 as an anti-MRSA agent: molecular docking, pharmacokinetics analysis, and molecular dynamic simulation studies. Saudi Pharm J. 2023;31(9):101744. doi: 10.1016/j.jsps.2023.101744, PMID 37649676.
18. Abraham MJ, Murtola T, Schulz R, Pall S, Smith JC, Hess B. Gromacs: high-performance molecular simulations through multi-level parallelism from laptops to supercomputers. Software X. 2015;1-2:19-25. doi: 10.1016/j.softx.2015.06.001.
19. Valdes Tresanco MS, Valdes Tresanco ME, Valiente PA, Moreno E. gmx_MMPBSA: a new tool to perform end-state free energy calculations with gromacs. J Chem Theory Comput. 2021;17(10):6281-91. doi: 10.1021/acs.jctc.1c00645, PMID 34586825.
20. Szklarczyk D, Kirsch R, Koutrouli M, Nastou K, Mehryary F, Hachilif R. The STRING database in 2023: protein-protein association networks and functional enrichment analyses for any sequenced genome of interest. Nucleic Acids Res. 2023;51(D1):D638-46. doi: 10.1093/nar/gkac1000, PMID 36370105.
21. Ritchie TJ, Macdonald SJF, Peace S, Pickett SD, Luscombe CN. Increasing small molecule drug developability in sub-optimal chemical space. Med Chem Comm. 2013;4(4):673-80. doi: 10.1039/c3md00003f.
22. Ottaviani G, Gosling DJ, Patissier C, Rodde S, Zhou L, Faller B. What is modulating solubility in simulated intestinal fluids? Eur J Pharm Sci. 2010;41(3-4):452-7. doi: 10.1016/j.ejps.2010.07.012, PMID 20656026.
23. Vinarov Z, Abdallah M, Agundez JAG, Allegaert K, Basit AW, Braeckmans M. Impact of gastrointestinal tract variability on oral drug absorption and pharmacokinetics: an UNGAP review. Eur J Pharm Sci. 2021;162:105812. doi: 10.1016/j.ejps.2021.105812, PMID 33753215.
24. Hollenberg PF. Characteristics and common properties of inhibitors, inducers, and activators of CYP enzymes. Drug Metab Rev. 2002 Jan;34(1-2):17-35. doi: 10.1081/dmr-120001387, PMID 11996009.
25. Kirchmair J, Goller AH, Lang D, Kunze J, Testa B, Wilson ID. Predicting drug metabolism: experiment and/or computation? Nat Rev Drug Discov. 2015;14(6):387-404. doi: 10.1038/nrd4581.
26. Mermer A, Vakal S. Pyrazine-chromene-3-carbohydrazide conjugates: molecular docking and ADMET predictions on dual-acting compounds against SARS-CoV-2 Mpro and RdRp. JRP 2021;25(6)(25(6)):953-66. doi: 10.29228/jrp.92.
27. Genheden S, Ryde U. The MM/PBSA and MM/GBSA methods to estimate ligand-binding affinities. Expert Opin Drug Discov. 2015;10(5):449-61. doi: 10.1517/17460441.2015.1032936, PMID 25835573.